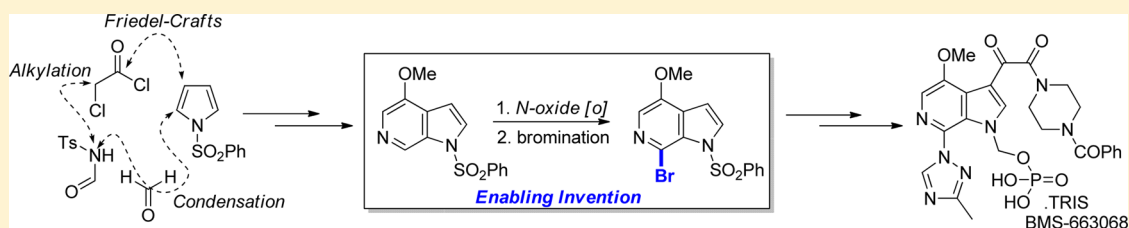


Synthesis of the 6-Azaindole Containing HIV-1 Attachment Inhibitor Pro-Drug, BMS-663068

Ke Chen, Christina Risatti, Michael Bultman, Maxime Soumeillant, James Simpson, Bin Zheng, Dayne Fanfair, Michelle Mahoney, Boguslaw Mudryk, Richard J. Fox, Yi Hsaio, Saravanababu Murugesan, David A. Conlon, Frederic G. Buono,[†] and Martin D. Eastgate*

Chemical Development, Bristol-Myers Squibb, 1 Squibb Drive, New Brunswick, New Jersey 08903, United States

S Supporting Information



ABSTRACT: The development of a short and efficient synthesis of a complex 6-azaindole, BMS-663068, is described. Construction of the 6-azaindole core is quickly accomplished starting from a simple pyrrole, via a regioselective Friedel–Crafts acylation, Pictet–Spengler cyclization, and a radical-mediated aromatization. The synthesis leverages an unusual heterocyclic *N*-oxide α -bromination to functionalize a critical C–H bond, enabling a highly regioselective copper-mediated Ullmann–Goldberg–Buchwald coupling to install a challenging triazole substituent. This strategy resulted in an efficient 11 step linear synthesis of this complex clinical candidate.

INTRODUCTION

For many patients infected with the HIV virus, treatment with the current antiretroviral therapies results in a high degree of viral suppression. However, there remains a need to develop new approaches to reduce viral replication with improved activity, mutant coverage, reduced side-effects, and alternate modes of action. The HIV-1 attachment inhibitor pro-drug,¹ BMS-663068 **1**,² is a compound currently in clinical development for the treatment of HIV infection (Figure 1).³ This

complexly functionalized 6-azaindole shows good activity and bioavailability when administered as the TRIS salt of the phosphate pro-drug.⁴ While this molecule may appear simple, its reactivity is dominated by electronic perturbations resulting from the interplay between the functional groups present on the aromatic nucleus. The disposition of functionality around the ring system has an impact on reactivity at each stage of the existing synthesis (Figure 1); for example, the C4-methoxy substituent significantly influences the reactivity at C7, complicating the installation of the triazole through standard S_NAr chemistry. The oxalate side-chain at C3 modifies the reactivity of the indole nitrogen (N1), which then affects N1/N6 regioselectivity during alkylation. Additional challenges result from the triazole itself, which is mildly acidic as a free compound (i.e., is a good leaving group), but once alkylated at nitrogen can be deprotonated at the ring carbon under basic conditions (deprotonation occurring at the methine). Furthermore, the three ring-nitrogen atoms of the triazole have competitive nucleophilic reactivity, leading to regioselectivity challenges during installation of this important fragment of the molecule. The existing synthesis (Figure 1), used to support clinical development, had several challenging steps, contained several safety liabilities, was long, and considered unsuitable for commercialization,⁵ despite several improvements made during development.⁶ This original synthesis started from 2-amino picoline **4** and required a significant number of challenging

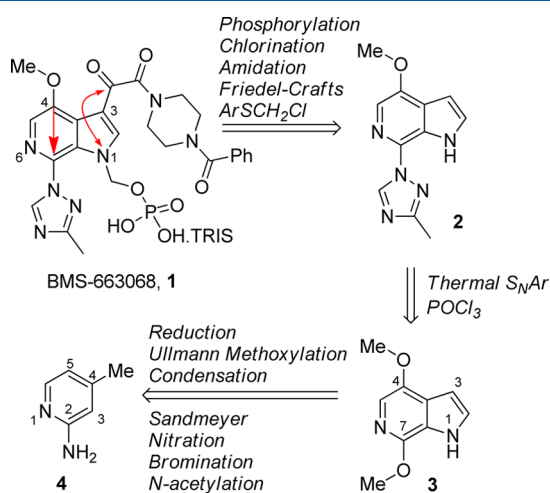


Figure 1. Key challenges and previous disconnection strategy.^{5,6}

Received: July 16, 2014

Published: August 21, 2014

transformations to reach the C4/7-dimethoxy-6-azaindole intermediate **3**; namely N-acetylation, C5-bromination, C3-nitration, Sandmeyer methoxylation, condensation of the C4-methyl group with dimethylformamide dimethyl acetal (DMF-DMA), Ullmann methoxylation (to install the methoxy group at C4 of the forming azaindole), reduction of the C3-nitro group (N1 of the azaindole), and finally, cyclization to form the 6-azaindole core (Figure 1). The installation of the triazole via this strategy was complicated by the early installation of the C4-methoxy moiety, which greatly deactivated C7 to S_NAr ; thus both the chlorination (neat $POCl_3/100\text{ }^\circ C$) and the subsequent triazole displacement ($140\text{ }^\circ C$ in 4-methyl-2-pentanol) required harsh reaction conditions, resulting in poor triazole N-selectivity (ca. 3:1:1). While selectivity was in favor of the desired isomer, the low selectivity resulted in a correspondingly modest isolated yield of the desired product **2** (ca. 56%). Finally, installation of the phosphate pro-drug was complicated by several handling and selectivity challenges.

During the initial development of this synthetic sequence several issues were observed with the pro-drug installation. To obviate these challenges the indole **2** was first N1-alkylated with $ArSCH_2Cl$ (the lack of acylation at C3 enabling high N1-selectivity), followed by Friedel–Crafts C3-acylation with methyl oxalyl chloride and amidation, to install the side-chain. Treatment with chlorine converted the N1 thio-ether to the N1 chloromethyl derivative (NCH_2Cl), which could then be treated with di-*tert*-butyl potassium phosphate to prepare the pro-drug in good yield. While this approach provided BMS-663068 **1**, the lengthy sequence, high number of complex steps and numerous safety liabilities led us to interrogate a completely different approach.

In reviewing alternate strategies for constructing the core of the molecule it was interesting to note that while 4, 5 and 7-azaindole derivatives have been known for some time, the 6-azaindole analogue is a relatively uncommon structure, with only a limited number of demonstrated synthetic approaches reported. The Bartoli cyclization⁷ of nitro pyridines can be used to prepare the 6-azaindole core, but it is a complex transformation, often resulting in poor yields.⁸ 3-Amino pyridine derivatives have also been used as starting materials through protection, lithiation, and condensation.⁹ This approach often intersects with 3-amino 4-picoline, which can be converted to a 6-azaindole through condensation of the methyl group with an appropriate formyl derivative (such as DMF-DMA) and subsequent cyclization.¹⁰ More complex strategies involving Pd-mediated cross-coupling and cyclization have also been developed.¹¹ While some of the palladium-mediated approaches appear, at first glance, to be appropriate in the context of azaindole **1**, we had to consider several complicating factors in designing our approach. BMS-663068 **1** was projected to require relatively high doses to reach efficacy targets in the clinic, thus synthetic efficiency and simplicity were prerequisites of any viable long-term synthesis. From the outset we realized that these additional constraints may rule out many Pd-mediated transformations (largely due to the use of either difficult to prepare ligand architectures or high catalyst loadings). While such limitations can be constrictive, this restriction can often be the catalyst for synthetic innovation. Thus, our approach to BMS-663068 **1** focused on a retrosynthetic hydrogenation of the 6-azaindole, approaching the synthesis from a lower oxidation state.¹² We believed that this strategy would enable a condensation-based approach, starting from a simple pyrrole, obviating the many challenges of

functionalizing pyridine analogues (Figure 2). During the course of this work, we discovered an unusual aromatization

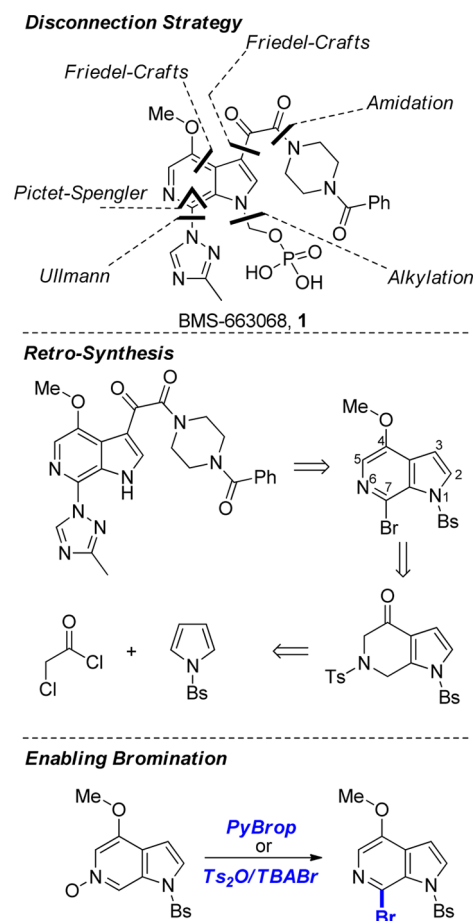


Figure 2. Disconnection proposal for BMS-663068 **1**.

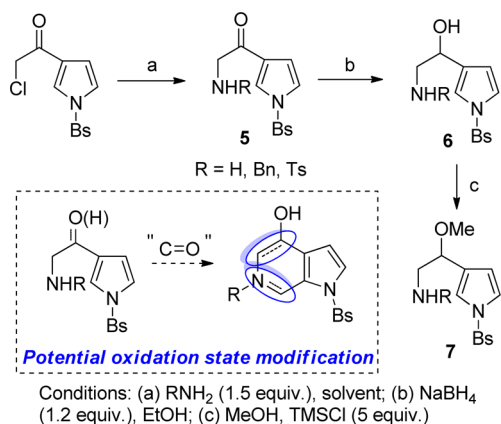
process, and invented a bromination protocol to functionalize heterocyclic pyridine *N*-oxides,¹³ which enabled the use of a highly regioselective Cu-mediated Ullmann–Goldberg–Buchwald coupling.¹⁴

RESULTS AND DISCUSSION

Assembly of the 6-Azaindole Core. To assess the viability of our proposed disconnection we prepared a range of amino-pyrroles, following a known C3-selective Friedel–Crafts acylation of *N*-benzenesulfonyl pyrrole with chloroacetyl chloride.¹⁵ Simple chloride displacement with a range of nitrogen sources gave a series of amino ketones **5** (Scheme 1) ready for further functionalization. Ketone reduction and optional methanolysis thus provided three viable substrate types (**5**, **6**, and **7**) for cyclization. We hoped that this strategy, through a combination of starting material oxidation state (i.e., ketone vs alcohol/ether) and condensing agent oxidation state (i.e., aldehyde, ester or carbonate), would allow us to target any desired oxidation state of the resulting azaindole (for example; 4,5-dihydro-, 6,7-dihydro-, or tetrahydro-azaindole) and potentially reveal additional options for installing both the methoxy at C4 and the triazole at C7.

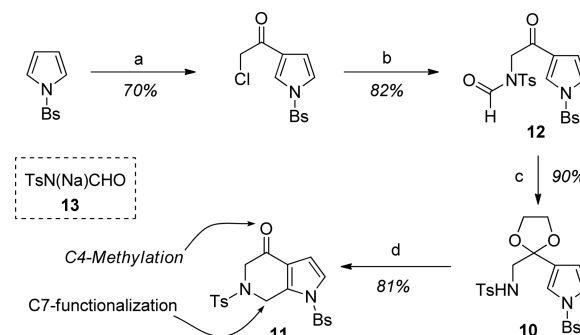
We initiated our study using ketone **5**, hoping to obtain cyclization while maintaining the oxidation level at C4, despite the obvious deactivation of pyrrole nucleophilicity the C3-carbonyl would induce. Unfortunately, Pictet–Spengler,¹⁶

Scheme 1. Preparation of Pyrrole-Based Amino-Alcohols



Bischler–Napieralski,¹⁷ or other common methods failed in the condensative cyclization. However, it was found that the lower oxidation state amino-alcohol derivatives (such as **6** and **7**) easily cyclized under standard Pictet–Spengler conditions (i.e., condensation with formaldehyde in dilute acid), forming the tetra-hydro azaindoles **8** and **9** in excellent yield (Scheme 2). We rationalized that sp^3 hybridization at C4 was critical for successful cyclization (potentially offering both electronic and conformational advantages), indeed, after initial ketalization of the C4 ketone **5** with ethylene glycol (to form dioxolane **10**), smooth cyclization was observed under standard Pictet–Spengler conditions to give 6,7-dihydroazaindole **11**; in this case cyclization was followed by *in situ* deprotection of the ketal post cyclization. Interestingly, only a Pictet–Spengler approach was effective in the cyclization, limiting us to producing the C6–C7 dihydro systems (by incorporation of a unit of formaldehyde). All attempts to affect cyclization at a higher oxidation state via Bischler–Napieralski or other similar processes (cyclizing amides, amidines, formates, etc.) resulted in nonproductive reactivity. With an understanding of the scope of the cyclization strategy, we investigated methods to further functionalize the tetrahydro derivatives (**8** and **9**). After exploring several unsuccessful methods to appropriately functionalize the tetrahydro-azaindoles, we focused on ketone **11** as the most promising substrate for downstream manipulation, hoping that the higher level of oxidation would ease the required aromatization process downstream. The optimized formation of this compound followed a simple 4 step

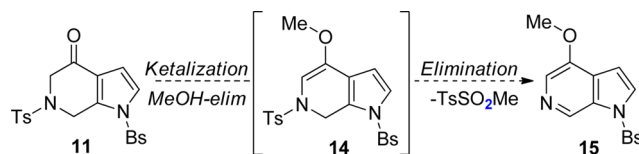
process (Scheme 3); after the initial Friedel–Crafts, displacement with sodium *N*-formyl tosylamide **13** gave ketone **12**,

Scheme 3. Optimized Synthesis of 6,7-Dihydroindole **11**

with the formyl group ensuring monoselectivity in the chloride displacement. Ketalization with ethylene glycol occurred with concurrent *N*-formyl deprotection, setting the stage for the Pictet–Spengler cyclization/deketalization, which occurred in excellent yield under mild conditions.

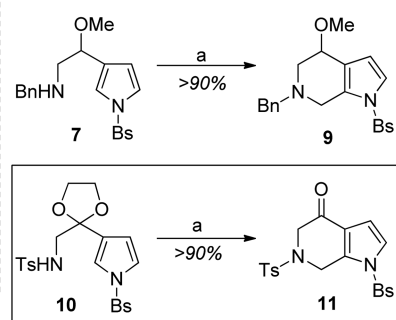
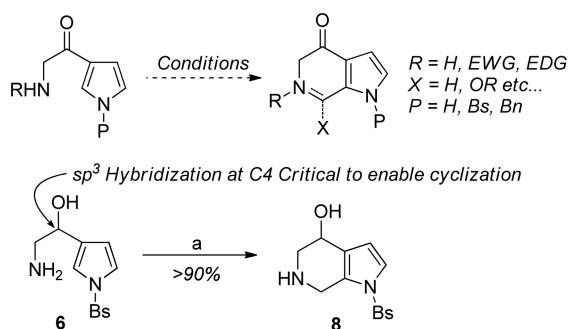
The tosylate protection of tetrahydroazaindole **11** was selected as it offered an additional functional handle for rearomatization, which we proposed could occur via a redox elimination (Scheme 4). It was envisaged that formation of the

Scheme 4. Initial Aromatization Conditions



corresponding methyl-enol **14** would facilitate thermal elimination of sulfinic acid, aromatizing the indole **15** (i.e.,

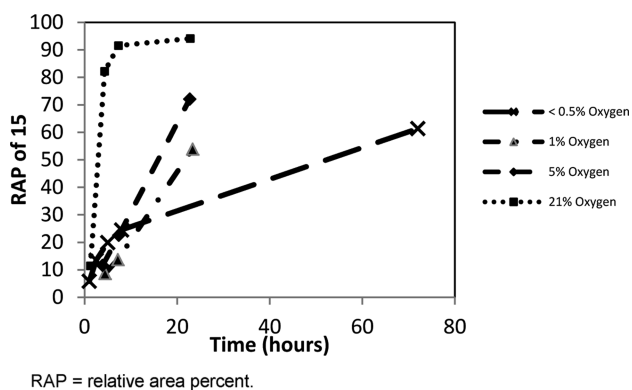
Scheme 2. Initial Interrogation of the Key Condensation To Form 6-Azaindoles



Conditions: (a) $(\text{CH}_2\text{O})_n$ (1.5 equiv.), TFA (2.0 equiv.), DCM (20 mL/g), rt. Note: yields are representative of small scale experiments using chromatography for isolation/purification.

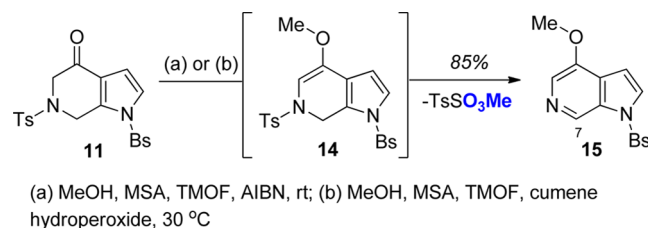
affecting reduction at sulfur with aromatic oxidation).¹⁸ After some experimentation, enabling conditions were identified, using 2,2-dimethoxypropane and ZrCl_4 as a Lewis-acid (where the zirconium promotes ketalization, enolization, and aromatization). While this reaction afforded excellent solution yields, the zirconium salts proved problematic to remove and resulted in significant loss of our desired product. After additional exploration, alternate conditions were found, leveraging protic acids or their anhydrides (such as MSA or Tf_2O with trimethyl orthoformate); however, both conditions were highly variable with reactions exhibiting great differences in reactivity. Some experiments would proceed rapidly to completion, while others would not progress past the intermediate enol ether **14**. After a detailed review of these results, we noted that the reaction performance correlated closely to the equipment used for the reaction, with poor performance in equipment which offered more tightly controlled environments (i.e., better inertness and removal of trace oxygen). The reaction was therefore performed under a strictly controlled atmosphere, with systematic variation of oxygen content ranging from <0.5% oxygen in nitrogen to atmospheric conditions (ca. 21% O_2) (Chart 1). These data showed that the rate of aromatization

Chart 1. Aromatization of **11** in the presence of varying levels of oxygen



was highly sensitive to oxygen content, with faster rates being observed in the presence of increasing oxygen concentrations. For example, the aromatization reaction reached 90+% conversion within 24 h under atmospheric conditions, while the reaction lingered around 60% conversion after 72 h with an oxygen content of <0.5%. Based on this information we hypothesized that the aromatization was a radical-based process. In order to avoid the complexity of using a controlled atmosphere in our chemistry (i.e., a set ratio of O_2/N_2), we chose to screen a variety of radical initiators to remove the sensitivity of the aromatization to oxygen. While AIBN, *tert*-butyl hydroperoxide and cumene hydroperoxide (CHP) were found to be highly competent mediators of the aromatization, we selected CHP as our optimal initiator due to its availability and ease of use (Scheme 5). However, as CHP rapidly undergoes the Hock Rearrangement under acidic conditions,¹⁹ we found it necessary to add the CHP in two portions to reliably get full conversion; indeed NMR analysis of the crude reaction mixture indicated that both phenol and acetone (the products of the Hock rearrangement of CHP) were formed in near quantitative amounts (based on the CHP input). Based on the limited data available, we believe this reaction is initiated through a minor decomposition pathway of CHP (either

Scheme 5. Optimized Conditions for the Preparation of **15**



through C–O or O–O bond homolysis), resulting in low concentrations of cumyl radical and/or peroxy radicals (the microscopic reverse of cumene hydroperoxide production),¹⁹ which then mediate the aromatization process. Interestingly, in contrast to the acidic thermal conditions, where methyl *p*-toluenesulfonate was produced as the stoichiometric byproduct, these conditions provided methyl *p*-toluenesulfonate as the elimination product (Scheme 5). This change appeared quantitative even though substoichiometric amounts of the initiators (AIBN or CHP) are used. With high yielding conditions for the aromatization in place, we turned our attention to functionalization of C7.

Introduction of the 3-Methyl-1,2,4-Triazole. The Reissert–Henze reaction is a common process used to functionalize the C2 position of pyridine, often proceeding through the corresponding pyridine *N*-oxide.²⁰ This process has been extended from the original addition of cyanide to include a wide range of *N*-oxide activators and nucleophilic partners.²¹ In our context, *N*-oxide **16** was easily prepared using standard conditions (methylrhodium trioxide (MTO)/ H_2O_2).²² While activation of the *N*-oxide **16**, under standard Reissert conditions (with tosic anhydride, in the presence of triazole **17**) showed high conversion and excellent solution yield, regioselectivity with respect to the triazole proved difficult to control (a 1:1 mixture of N1:N2 (**18**:**19**) was generally observed, with coupling at N4 only a minor product, Table 1). We rationalized that the poor regioselectivity was induced by the competition of electronic and steric influences on the triazole. We therefore designed a survey of indole nitrogen protecting groups and activating agents, to determine if variations within either the electrophilic partner or activating agent could improve the regioselectivity observed in the addition (Table 1). Electron-poor *N*-protecting groups (i.e., Boc, benzenesulfonyl, Piv) showed poor regiochemical control, with little variance from a 1:1 N1:N2 ratio. In this series the activating agent had little effect, though it was evident that chloride was a competitive nucleophile to the triazole. More electron-neutral *N*-substituents (i.e., Bn, MOM, phosphate) showed only a slight improvement in regioselectivity, with *N*-Bn providing a 2.8:1 ratio in favor of the desired isomer **18**. While this is only modest selectivity, isolation of the desired isomer in a pure form was easily achieved (~56% overall yield). Despite these low yields, this approach was competitive with the conditions used in the previous approach (which used high temperatures and long reaction times to produce similar results in terms of yield and selectivity, *vide supra*).

While we had accomplished the desired C7-functionalization, the outcome was less than satisfactory. During our work on this transformation, Londregan et al. published their findings using the coupling agent PyBroP^{23} as an activator in Reissert–Henze chemistry.²⁴ This system demonstrated reactivity across a wide range of oxygen and nitrogen-based nucleophiles and appeared to offer a new approach to activation, as such, we explored

Table 1. Reissert Addition of Triazole 17 to *N*-Oxide 16

16

17

Desired
18

Undesired
19

7-Cl adduct
20

N¹: Most sterically accessible
N²: Most electron-rich

R = Electron Withdrawing				R = Electron Donating			
R Group	Reagent	18:19	20	R Group	Reagent	18:19	20
	Ts ₂ O, TEA	1.3 : 1	N/A		BsCl	1.9 : 1	ca. 21%
	TsCl, TEA	1.3 : 1	N/A		MsCl	2.7 : 1	ca. 54%
	BsCl	1 : 1	ca. 20%		Ms ₂ O ^a	2.8 : 1	N/A
	Tf ₂ O	1 : 1	N/A		Bs ₂ O	2.2 : 1	N/A
	BsCl/Et ₃ N	1 : 1	ca. 20%		Ts-triazole	1.9 : 1	N/A
	Ac ₂ O	1 : 1	N/A		BsCl	2 : 1	ca. 35%
Bs ₂ O	1 : 1	N/A	TsCl		2 : 1	ca. 24%	
	TsCl	1.25 : 1	ca. 13%		Ms ₂ O	1.7 : 1	N/A
					Bs ₂ O	1.9 : 1	N/A
					BsCl, DIPEA	1.3:1	N/A

^aProvided 56% isolated yield as a single isomer.Table 2. Bromination screen of *N*-Oxide 16

conditions	21 (%) ^a	22 (%) ^a	15 (%) ^a	note
POBr ₃	trace	trace	trace	decomposition
PPh ₃ /Br ₂	11	5	79	rt or 50 °C
PPh ₃ /NBS	25	3	69	rt or 50 °C
AcBr	N/A	N/A	95	clean reaction
PhSO ₂ Br	40 AP	N/A	46	DCM, rt, 12 h
PyBroP	82 AP (80%) ^b	N/A	10	K ₃ PO ₄ , PhCF ₃ , rt, 6 h

^aRelative area percent determined by HPLC. ^bSolution yield of a gram-scale experiment.

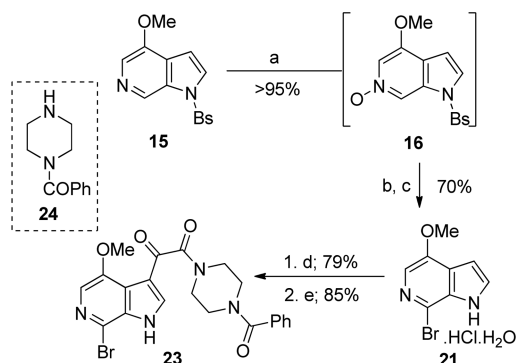
these conditions in our triazole coupling. While triazole regioselectivity was again poor, analysis of the reaction mixture showed some evidence of C7-bromination under the PyBroP-mediated conditions. Intrigued by the possibilities of a C7-bromide in the downstream chemistry, we focused on optimizing this side reaction. Simply removing the triazole 17 and optimizing base, solvent, and temperature resulted in a good yields (ca. 70–80%) of the C7-bromide 21 (Table 2). To the best of our knowledge, this reactivity of pyridine-like *N*-oxides is unprecedented, indeed C2-bromopyridines are significantly more challenging to prepare than their chloride analogues. Typically, pyridine-2-ones react smoothly with POCl₃ to prepare 2-Cl pyridines, whereas significantly more forcing conditions are required to effect bromination (i.e., using POBr₃ or a combination of P₂O₅/TBABr at high temperature).²⁵ Indeed, when POBr₃ was used in place of POCl₃ in our original synthesis (Figure 1) it proved challenging to produce even modest amounts of the corresponding bromide

21.²⁶ To compare PyBroP to other standard bromination systems, a wide range of alternate conditions were surveyed using *N*-oxide 16, such as NBS/PPh₃,²⁷ POBr₃,²⁸ PPh₃/Br₂ among others (Table 2), all these approaches led mainly to des-oxygenation (i.e., recovery of 15), while PyBroP was the exception and appeared unique in its ability to smoothly brominate this azaindole *N*-oxide 16. Further interrogation of these enabling conditions resulted in the development of a Ts₂O/TBABr(Cl) based process for the bromination (or chlorination) of heterocyclic *N*-oxides, chemistry which was recently reported.²⁹

The ability to prepare the C7-bromide 21 suggested exciting possibilities to improve the triazole installation, not only opening up the potential to install the triazole later in the sequence (avoiding impurities formed through the acidic C–H on the triazole), but also enabling the use of a ligated Cu-mediated process (such as an Ullmann–Goldberg–Buchwald reaction), which we hoped would improve the regiochemical

outcome of the addition.³⁰ With this goal in mind, we prepared the amide **23**, through *N*-benzenesulfonyl deprotection, Friedel–Crafts acylation/hydrolysis and amidation with piperazine **24**³¹—all of which proceeded in high yield (Scheme 6).

Scheme 6. Preparation of the Amide **23**



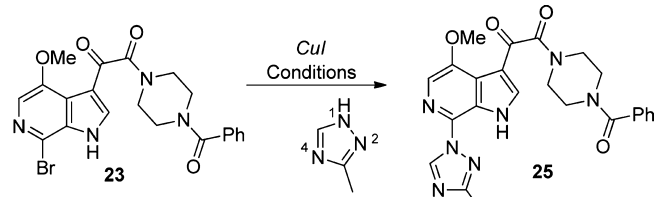
Conditions: (a) MTO (0.2 mol%), H₂O₂ (2.0 equiv.), DCM; (b) PyBrOP (1.2 equiv.), K₃PO₄ (2 equiv.), trifluorotoluene; (c) aq. NaOH, IPA; (d) MeO₂CCOCl (2.0 equiv.), AlCl₃ (4.3 equiv.), DCM/MeNO₂ then NaOH; (e) CDI (1.1 equiv.), **24** (1.0 equiv.), DMF.

With the key amide **23** in hand, we studied the late-stage installation of the triazole **17**.³² Extensive screening was carried out for the Ullmann–Goldberg–Buchwald coupling, investigating the choice of ligand, base, solvent, and metal precursor. Our initial screens mainly focused on the use of diamine,³³ diketone,³⁴ and phenanthroline³⁵ ligands, among others; some of our initial results are shown (Table 3). It was found that in the presence of copper iodide (a preferred catalyst precursor), the 1,2-diamine ligands were unique in their reactivity and were significantly better than other ligand classes; *trans*-DMCHDA (*trans*-dimethyl cyclohexyl diamine) proved especially effective. We were pleased to find in our initial leads, especially with diamino-ligands, that greatly improved regioselectivities were generally observed vs the thermal S_NAr approach (*vide supra*);

up to a 10:1 N1/N2 ratio was obtained in the initial test reactions with *trans*-DMCHDA. We presumed that this was due to a much tighter transition state induced by the catalytic process (Figure 3). The coupling generally performed well in most organic solvent classes (such as hindered alcohols, acetates, ethers and nitriles), though the nature of the cationic component of the base proved critical. Potassium was uniquely effective (Li or Na cationic counterions provided little to no observable product), interestingly the anionic component of the base was much less significant. Utilization of either *t*BuOK or K₂CO₃ provided similar results, which were comparable to the use of preformed potassium-triazolate. Intriguingly, it was discovered that the presence of water significantly enhanced both reactivity and regioselectivity. The reason for this effect is unknown, though the impact of water on the rate of Ullmann couplings has been documented elsewhere.³⁶ Consequently, replacing *t*BuOK with aqueous KOH, provided the required counterion, base and water, which, along with further optimization, delivered a reproducible and highly regioselective process (>20:1 N1/N2 isomeric ratio and >80% in-process yield). To isolate the desired product, LiBr was added (after a simple aqueous workup) effecting *in situ* salt metathesis and crystallization of a highly crystalline Li-salt of **25**, isolated as a KBr cocrystal (Scheme 7).

Pro-Drug Formation. The conversion of Li-salt **25** to BMS-663068 **1** involves only pro-drug installation, however, the installation of the phosphate was not without complexity. Previously, thiomethylation, chlorination, and phosphate displacement had been used to prepare **26**, this lengthy sequence was conducted to obviate issues of reactivity and reagent availability, involved in the direct alkylation.^{5,6} In reconsidering the installation of the last section of the molecule, we wished to return to a direct alkylation-based approach, utilizing a chloromethyl-phosphate derivative such as phosphate ester **27**. In order to accomplish this strategic revision, concurrent development of new methods to prepare both the chloromethyl-phosphate electrophile **27**³⁷ and its starting material, chloromethyl chlorosulfate,³⁸ were developed. The

Table 3. Optimization of the Ullmann–Goldberg–Buchwald reaction



ligand	ligand equiv	CuI equiv	base	solvent	conversion ^a (yield)	N1/N2
phenanthrene ^b	5	0.5	KO ^t Bu	4-methyl-2-pentanol.	0	N/A
2,2-bipyridine	5	0.5	KO ^t Bu	4-methyl-2-pentanol	0	N/A
8-quinolinol	5	0.5	KO ^t Bu	4-methyl-2-pentanol	0	N/A
EDTA or MIDA	5	0.5	KO ^t Bu	4-methyl-2-pentanol	0	N/A
DMEDA	1.5	0.2	KO ^t Bu	4-methyl-2-pentanol	37%	4:1
DMCHDA ^c	1.5	0.2	KO ^t Bu	4-methyl-2-pentanol	90%	10:1
DMCHDA	5	0.5	LiOH or Na ₂ CO ₃ ^d	4-methyl-2-pentanol	<5%	N/A
DMCHDA	1.5	0.2	KO ^t Bu or K ₂ CO ₃	THF or EtOAc or MeCN	85–93%	10:1
DMCHDA	1.5	0.2	KO ^t Bu; 10 equiv H ₂ O	MeCN	>98%	>20:1
DMCHDA	1.5	0.2	aq KOH	MeCN	>98% (85%) ^e	22:1

^aConversion was based on reactions run at 80 °C over 20 h. ^bVarious phen-type ligands were tested, all of which failed to promote the coupling. ^cDMCHDA; *N,N*-dimethyl-1,2-cyclohexanediamine. ^dOrganic bases such as pyridine or Hunig's base also failed to promote the coupling. ^eSolution yield obtained from a 2 g-scale experiment.

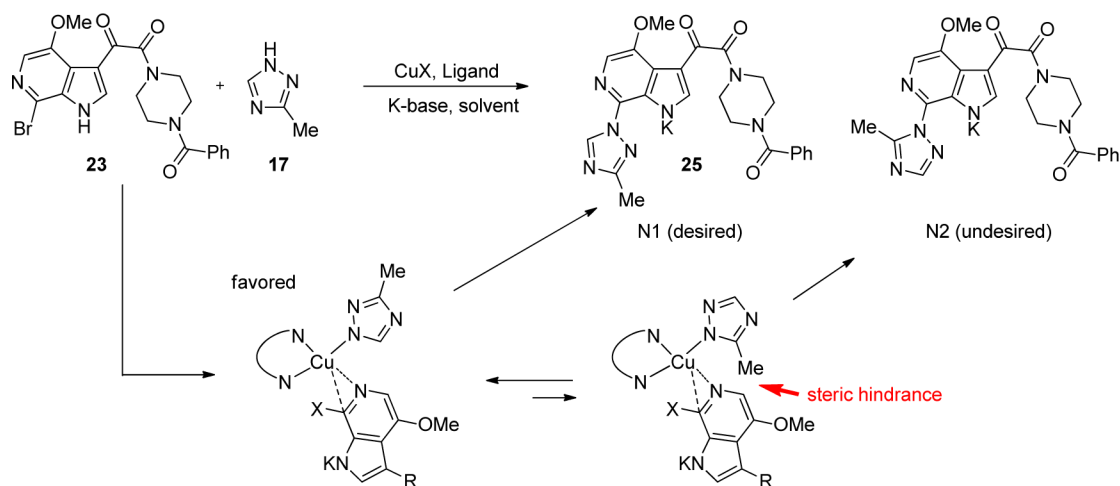
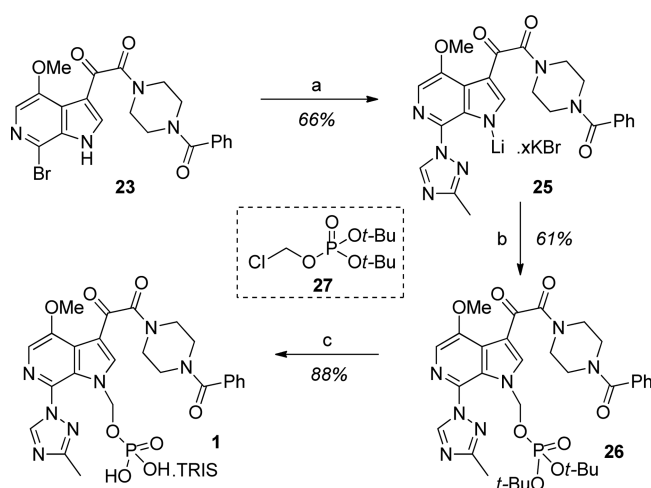


Figure 3. Proposed rationale for regioselectivity in the Ullmann–Goldberg–Buchwald coupling of bromide 23 to triazole 17.

Scheme 7. End-Game Steps To Prepare BMS-663068, 1



Conditions: (a) **17** (1.5 equiv.), CuI (20 mol%), DMCHDA (1.5 equiv.), KOH (aq., 2.1 equiv.), MeCN, then LiBr (1.1 equiv.); (b) **27** (1.3 equiv.), K_3PO_4 (1.0 equiv.), Et_4NI (0.5 equiv.), MeCN; (c) acetone, water, tromethamine.^{2b}

protio-form of **25** had been utilized in an alkylation with phosphate **27** previously, as part of an earlier synthesis of this BMS-663068 **1**.^{2b} In that case, alkylation occurred with modest yield and N1 to N6-selectivity. During optimization of this reaction we screened a range of alternate salt forms of **25**; for example, *tetra*-butyl ammonium and potassium salts. While, none of these alternate forms provided crystallinity in the azaindole **25**, all showed reactivity with the chloromethyl-phosphate **27**. However, surprisingly the lithium salt, while providing an isolatable crystalline form of **25**, was much less reactive in the alkylation; presumably due to the lithium counterion preferring to coordinate (and therefore localize charge) in the conjugated α -keto amide, as opposed to direct nitrogen coordination and charge localization. Thus, *in situ* salt metathesis from lithium to potassium was required for productive alkylation. After extensive screening, we discovered that the use of wet acetonitrile (KF = 1%) as solvent, in the presence of 0.5 equiv of tetraethylammonium iodide (to facilitate an *in situ* halide exchange) and either tribasic potassium phosphate or potassium carbonate as additives, led to efficient conversion of **25** to **26**. Interestingly, the use of wet

solvent was critical, and alternative potassium additives (i.e., dibasic phosphate, bicarbonate, acetate, benzoate, formate, etc.) led to poor reactivity. Our analysis of this trend suggested that potassium additives with significantly less soluble lithium analogues were critical for driving the salt metathesis process in the desired direction. With *tert*-butyl phosphate **26** in-hand, deprotection was accomplished under previously reported conditions, to give the final compound in excellent purity.^{2b}

Overall, this new synthesis provided BMS-663068 **1** in 11 linear steps and 5.9% overall yield, setting the stage for further optimization of this strategy for the potential manufacture of BMS-663068 on commercial scales. The transformations described herein have been subsequently optimized and improved, to provide the manufacturing route to BMS-663068 **1**, with significant additional yield improvements. This work will be described in due course.

CONCLUSION

An efficient synthesis of a complex 6-azaindole, BMS-663068, has been accomplished in an 11-step sequence from simple precursors such as pyrrole and 3-methyl-1H-1,2,4-triazole. The route features the rapid assembly of a 6-azaindole, leveraging a low oxidation state approach via a condensative cyclization, followed by a radical-mediated redox-aromatization to reveal the 6-azaindole. Other highlights include an unusual α -bromination of a heterocyclic *N*-oxide, which provides a critical functional handle for a highly regioselective Ullmann–Goldberg–Buchwald coupling to install the key triazole moiety.

EXPERIMENTAL SECTION

2-Chloro-1-(1-(phenylsulfonyl)-1H-pyrrol-3-yl)ethanone.¹⁵

Aluminum chloride (21.2 g, 1.1 equiv) and dichloromethane (300 mL) were added to a 500 mL round-bottom flask under an atmosphere of nitrogen. Chloro acetyl chloride (12.6 mL, 1.1 equiv) was then added in one portion, at which point the reaction turned from white slurry into a light-yellow homogeneous solution. After stirring at ambient temperature for 10 min, *N*-benzenesulfonylpyrrole (30 g, limiting reagent) was added in 2–3 portions over 30 min. The resulting brown solution was stirred overnight. After cooling to 0 °C, aq sodium bicarbonate (10 wt %, 250 mL) was added slowly while maintaining the internal temperature below 20 °C. The biphasic mixture was stirred for 30 min, and the layers were separated. The organic layer was dried over sodium sulfate, filtered, and concentrated under vacuum to afford a dark-brown oil. Purification by silica-gel chromatography (eluting with 10–30% EtOAc in hexanes) afforded the 3-acyl-pyrrole

as a white crystalline solid (29 g, 70% yield). R_f = 0.6 in 25% EtOAc in hexanes; mp = 105–106 °C; ^1H NMR (500 MHz, CDCl_3) δ : 7.91 (d, J = 7.6 Hz, 2 H), 7.86 (s, br, 1 H), 7.66 (t, J = 7.32 Hz, 1 H), 7.55 (dd, J = 7.3, 7.6 Hz, 2 H), 7.17 (s, br, 1 H), 6.71 (s, br, 1 H), 4.45 (s, 2 H); ^{13}C NMR (125 MHz, CDCl_3) δ : 186.1, 137.6, 134.7, 129.7 (2), 127.1 (2), 125.6, 124.9, 121.8, 112.4, 46.0; HRMS [M – H; ESI-ORBITRAP] calcd for $\text{C}_{12}\text{H}_9\text{ClNO}_3\text{S}$: 281.9986; found: 281.9979.

Sodium *N*-tosylformamide, 13.³⁹ A mixture of sodium methoxide in methanol (25% w/w, 300 mL, 1.5 equiv) and toluene sulfonamide (150 g, limiting reagent) was heated to 30 °C for 30 min, at which point a thick slurry (sodium tosylamide) formed. Methanol (200 mL) was added, followed by portion-wise addition of ethyl formate (282 mL, 4 equiv). The resulting mixture was stirred vigorously at 30 °C while the reaction conversion was monitored by HPLC. Upon completion (typically 14 h), the reaction mixture was cooled to 20 °C, filtered, washed with methanol (450 mL) and dried in vacuum at 50 °C to afford sodium *N*-tosylformamide 13 as a white solid (183.3 g, 83%). HPLC monitored at 256 nm using Water Symmetry Shield RP-8, 3.5 mm 4.6×150 mm column, gradient method: 10% B (0 min) to 100% B (12 min), then 100% B (15 min). Mobile phase A: water (80%), methanol (20%) with 0.05% trifluoroacetic acid, Mobile phase B: acetonitrile (80%), methanol (20%) with 0.05% trifluoroacetic acid. HPLC retention time: 8.35 min. Melting point (mp) = 261 °C; ^1H NMR (400 MHz, $\text{DMSO}-d_6$) δ : 8.75 (br s, 1H), 7.52 (d, br, J = 8.3 Hz, 2H) 7.22 (d, br, J = 7.8 Hz, 2H) 2.32 (s, 3 H); ^{13}C NMR (100 MHz, $\text{DMSO}-d_6$) δ : 170.0, 144.2, 139.6, 128.7 (2), 125.4 (2), 20.8; HRMS [M + H; ESI-ORBITRAP] calcd for $\text{C}_8\text{H}_{10}\text{NO}_3\text{S}$: 200.0381; found: 200.0379.

***N*-(2-oxo-2-(1-(phenylsulfonyl)-1H-pyrrol-3-yl)ethyl)-*N*-tosylformamide, 12.** To a slurry of sodium *N*-tosylformamide 13 (9.36 g, 1.2 equiv) in THF (100 mL) was added tetra-*N*-butylammonium iodide (1.3 g, 0.1 equiv) and the chloro-ketone (10.0 g, limiting reagent). The reaction was heated to 60 °C for 3 h, at which point reaction completion was determined via HPLC. The solution was then cooled to 20 °C and washed with hydrochloric acid (0.5 M, 50 mL) and then sodium chloride solution (25% w/w, 50 mL). The collected organic layer was concentrated to ca. 60 mL, at which point isopropyl alcohol was added (57 mL). After stirring at ambient temperature for 20 min, additional isopropyl alcohol was added (57 mL), and the resulting slurry was cooled to 10 °C to enable crystallization. After stirred at 10 °C for another 20 h, the product was filtered, washed with isopropyl alcohol/THF (50/50, 3×30 mL), and dried under vacuum at 50 °C to afford *N*-(2-oxo-2-(1-(phenylsulfonyl)-1H-pyrrol-3-yl)ethyl)-*N*-tosylformamide 12 as a white solid (12.95 g, 82%). HPLC at 256 nm using Water Symmetry Shield RP-8, 3.5 mm 4.6×150 mm column, gradient method 10% B (0 min) to 100% B (12 min), then 100% B (15 min), Mobile phase A: water (80%), methanol (20%) with 0.05% trifluoroacetic acid, Mobile phase B: acetonitrile (80%), methanol (20%) with 0.05% trifluoroacetic acid, HPLC retention time: 11.90 min. Melting point (mp) = 142 °C; ^1H NMR (500 MHz, CDCl_3) δ : 9.14 (br s, 1H), 7.92 (d, br, J = 8.7 Hz, 2H) 7.76–7.75 (m, 3H) 7.69 (t, J = 6.6 Hz, 1H) 7.58 (t, J = 7.6 Hz, 2H) 7.35 (d, br, J = 8.5 Hz, 2H) 7.16 (dd, J = 3.2, 2.2 Hz, 1H) 6.62 (dd, J = 3.5, 1.6 Hz, 1H) 4.75 (s, 2H) 2.46 (s, 3H); ^{13}C NMR (126 MHz, CDCl_3) δ : 184.4, 160.7, 145.7, 137.8, 134.8, 134.7, 130.1 (2), 129.8 (2), 127.7 (2), 127.3 (2), 125.5, 124.3, 121.8, 112.1, 48.2, 21.7; HRMS [M + H; ESI-ORBITRAP] calcd for $\text{C}_{20}\text{H}_{19}\text{N}_2\text{O}_6\text{S}_2$: 447.0679; found: 447.0669.

4-Methyl-*N*-((2-(1-(phenylsulfonyl)-1H-pyrrol-3-yl)-1,3-dioxolan-2-yl)methyl)benzenesulfonamide, 10. To a mixture of *N*-(2-oxo-2-(1-(phenylsulfonyl)-1H-pyrrol-3-yl)ethyl)-*N*-tosylformamide 12 (10.1 g, 22.4 mmol) and methanol (100 mL) was added a methanolic sulfuric acid solution (4.5 mL, 2.23 mmol). [Note: The H_2SO_4 -MeOH was prepared by dissolving H_2SO_4 (96 wt %, 0.228 g, 2.23 mmol) in MeOH (3.44 g).] The reaction was warmed to 60 °C and stirred for 3h. Ethylene glycol (13.9 g, 10 equiv) was then added, followed by trimethyl orthoformate (7.26 g, 3 equiv). As the reaction progressed, 4-methyl-*N*-((2-(1-(phenylsulfonyl)-1H-pyrrol-3-yl)-1,3-dioxolan-2-yl)methyl)benzenesulfonamide 10 crystallized from solution. Once complete reaction was observed (typically 1 h), the

reaction mixture was cooled to 20 °C and aged for 1 h to afford a thick slurry. The product was filtered, washed with methanol (80 mL), and dried under vacuum at 60 °C to afford dioxolane 10 (9.56 g, 97.2 wt %, 90% yield). HPLC at 232 nm using Ascentis Express C18 2.7 μm 4.6×50 mm column, gradient method 40% B (0–4.5 min) to 100% B (6 min). Mobile phase A: 0.01% NH_4OAc in H_2O : MeOH (80:20), Mobile phase B: 0.01% NH_4OAc in H_2O : MeOH: CH_3CN (5:20:75). Retention time: 3.0 min. Melting point (mp) = 188–199 °C; ^1H NMR (500 MHz, CDCl_3) δ : 7.9 (d, J = 7.5 Hz, 2 H), 7.7 (d, J = 7.8 Hz, 2 H), 7.6 (t, J = 7.5 Hz, 1 H), 7.5 (t, J = 7.5 Hz, 2 H), 7.2 (s, br, 2 H), 7.1 (s, 1 H), 7.0 (s, 1 H), 6.2 (s, 1 H), 4.7 (s, br, 1 H), 3.9 (s, br, 2 H), 3.8 (s, br, 2 H), 3.2 (d, J = 6.1 Hz, 2 H), 2.4 (s, 3 H). ^{13}C NMR (125 MHz, CDCl_3) δ : 143.30, 138.71, 137.31, 134.11 (2), 129.58 (2), 129.53 (2), 128.48, 127.00 (2), 126.91 (2), 118.67, 111.70, 105.47, 65.35 (2), 49.35, 21.53. $\text{CHNC}_{21}\text{H}_{22}\text{N}_2\text{O}_6\text{S}_2$: calcd: 54.53% C, 4.79% H, 6.06% N; found: 54.53% C, 4.88% H, 5.93% N. HRMS [M + H; ESI-ORBITRAP] calcd for $\text{C}_{21}\text{H}_{23}\text{N}_2\text{O}_6\text{S}_2$: 463.0992; found: 463.0989.

1-(phenylsulfonyl)-6-tosyl-6,7-dihydro-1H-pyrrolo[2,3-*c*]pyridin-4(5H)-one, 11. To a slurry of dioxolane 10 (10.00 g, limiting reagent) and paraformaldehyde (1.6 g) in dichloromethane (100 mL) at 20 °C was added trifluoroacetic acid (4.90 mL, 3 equiv). Once the reaction was complete (typically 2 h), the reaction was quenched with aqueous solution of dibasic potassium phosphate (10 wt %, 100 mL) and further stirred for 20 min. The aqueous layer was discarded, and the organic layer was polished filtered to remove remaining paraformaldehyde. The organic layer was then concentrated to ca. 50 mL, at which point isopropyl acetate (24 mL) and methyl *tert*-butylether (30 mL) were added. The solution was distilled with constant methyl *tert*-butylether addition to remove dichloromethane. The resulting slurry was then cooled to 0 °C over a course of 2 h. The product was filtered, washed with methyl *tert*-butylether (2×50 mL), and dried at 50 °C in a vacuum oven to give 1-(phenylsulfonyl)-6-tosyl-6,7-dihydro-1H-pyrrolo[2,3-*c*]pyridin-4(5H)-one 11 as a white solid (7.56 g, 81%). HPLC at 230 nm using Phenomenex Kinetex, C18 100A, 4.6×150 mm column with gradient method 15% B (0 min) to 60% B (20 min) to 100% B (25 min) then 100% B (30 min). Mobile phase A: water (80%), methanol (20%) with 0.01 M NH_4OAc . Mobile phase B: acetonitrile (75%), methanol (15%), water (5%) with 0.01 M NH_4OAc , retention time: 20.33 min; Melting point (mp) = 168 °C; ^1H NMR (500 MHz, CDCl_3) δ : 8.01 (dd, J = 8.4, 3.0 Hz, 2H), 7.78 (dt, J = 5.3, 1.2 Hz, 1H), 7.68 (t, J = 7.8 Hz, 2H), 7.30 (d, J = 8.4 Hz, 2H), 7.14 (d, J = 3.5 Hz, 1H), 7.07 (d, J = 8.1 Hz, 2H), 6.39 (d, J = 3.3 Hz, 1H), 4.85 (s, 2H), 3.95 (s, 2H) 2.33 (s, 3H); ^{13}C NMR (125 MHz, CDCl_3) δ : 187.0, 144.1, 137.9, 137.5, 135.3, 134.0, 130.2 (2), 129.8 (2), 127.4 (2), 127.1 (2), 122.7, 122.5, 108.3, 53.0, 43.2, 21.5; HRMS [M + H; ESI-ORBITRAP] calcd for $\text{C}_{20}\text{H}_{19}\text{N}_2\text{O}_5\text{S}_2$: 431.0730; found: 431.0722.

4-Methoxy-1-(phenylsulfonyl)-1H-pyrrolo[2,3-*c*]pyridine, 15. Ketone 11 (10 g, limiting reagent), methanol (120 mL), and methanesulfonic acid (2.9 g, 1.5 equiv) were sequentially charged to a 250 mL round-bottom flask. The mixture was then heated to 30 °C. Trimethylorthoformate (10.5 g, 5 equiv) was added, followed by cumene hydroperoxide (1.5 g, 0.5 equiv in two equal portions, 1 h apart). The reaction progress was monitored by HPLC. Upon completion (typically 2 h), the crude mixture was cooled to 20 °C. Triethylamine (3.4 g, 1.7 equiv) was slowly added over a course of 30 min. Aqueous sodium thiosulfate (1 wt %, 100 mL) was slowly added over the course of 2 h, resulting in the formation of a thick slurry. The product was filtered, washed with water/methanol (45/55; 50 mL), and then dried under vacuum at 50 °C. Azaindole 15 was isolated as a white crystalline solid (4.9 g, 85% yield). HPLC at 230 nm using Phenomenex Kinetex, C18 100A, 4.6×150 mm column gradient method 15% B (0 min) to 60% B (20 min) to 75% B (25 min). Mobile phase A: water (80%), methanol (20%) with 0.01 M NH_4OAc . Mobile phase B: acetonitrile (75%), methanol (15%), water (5%) with 0.01 M NH_4OAc , retention time: 15.19 min; Melting point (mp) = 152 °C; ^1H NMR (500 MHz, CDCl_3) δ : 9.01 (s, 1H), 8.03 (s, 1H), 7.92 (m, 2H), 7.68 (d, J = 3.9 Hz, 1H), 7.60 (dt, J = 7.8, 1.0 Hz, 1H), 7.49 (dt, J = 8.3, 1.9 Hz, 2H), 6.84 (d, J = 3.0 Hz, 1H), 4.00 (s, 3H); ^{13}C NMR

(125 MHz, CDCl₃) δ : 149.6, 137.5, 134.5, 132.3, 129.6 (2), 129.1, 128.1, 127.6, 126.9 (2), 122.8, 105.6, 56.3; HRMS [M + H; ESI-ORBITRAP] calcd for C₁₄H₁₃N₂O₃S: 289.0641; found: 289.0639.

7-Bromo-4-methoxy-1H-pyrrolo[2,3-c]pyridine hydrochloride salt monohydrate, 21. *N*-Oxidation. To a solution of azaindole 15 (10 g, limiting reagent) in dichloromethane (200 mL) at 25 °C was added hydrogen peroxide (6.1 mL, 35 wt %, 2 equiv) followed by MTO (17 mg, 0.2 mol %). The mixture was stirred at 25 °C until reaction reached completion by HPLC monitoring (typically 24 h). If needed, additional 0.2 mol % MTO was added to drive reaction to completion. The mixture was cooled to 0 °C and quenched with aq sodium sulfite solution (20 wt %, 50 mL). The layers were separated, and the product-rich lower DCM layer was washed with water (50 mL). The collected DCM solution was diluted with trifluorotoluene (100 mL). The resulting thin slurry was distilled with constant trifluorotoluene addition until residual DCM was <1 vol % by GC analysis. Adjust the overall volume of the reaction crude to ca. 150 mL, and submit the thick slurry to the subsequent bromination/hydrolysis step without further purification.

Bromination. To a slurry of *N*-oxide 16 in trifluorotoluene (ca. 150 mL) at 20 °C was added K₃PO₄ (36.5 g, 5 equiv) and PyBroP (19.3 g, 1.1 equiv). The resulting mixture was stirred at 20 °C for 3 h, then warmed to 50 °C, and stirred at that temperature until bromination reached completion by HPLC analysis (typically 2 h).

Hydrolysis. IPA (80 mL) was then added, followed by aqueous sodium hydroxide (2 N, 80 mL). The mixture was warmed to 80 °C and stirred at that temperature. Upon completion of hydrolysis by HPLC analysis (typically 12 h), the reaction was cooled to 20 °C. The upper organic phase was separated and distilled under reduced pressure (150–200 Torr, 50 °C) to ~100 mL. The resulting slurry was filtered to remove residual inorganics. The temperature was adjusted to 50 °C, at which point HCl/IPA (5 N, 10 mL, 1.5 equiv) was added. The resulting slurry was stirred at 50 °C for 30 min, then cooled to 5 °C over 2 h, and maintained at 5 °C overnight. The product was collected by filtration and dried at 50 °C for 12 h to afford bromide 21 as its HCl salt monohydrate (7.0 g, 70% yield). HPLC at 256 nm using YMC Pro C18 3 μ m 4.6 \times 150 mm column with a gradient method: 20% B (0–1 min) to 55% B (10 min), then 100% (16.5 min). Mobile phase A: water with 0.05% trifluoroacetic acid. Mobile phase B: acetonitrile with 0.05% trifluoroacetic acid, retention time: 5.31 min. Decomposed at 160 °C; ¹H NMR (500 MHz, DMSO-*d*₆) δ : 12.80 (s, 1 H), 7.84 (s, br, 1 H), 7.68 (s, 1 H), 6.99 (s, br, 4 H), 6.73 (s, br, 1 H), 3.97 (s, 3 H); ¹³C NMR (125 MHz, DMSO-*d*₆) δ : 149.8, 133.7, 131.8, 126.8, 115.8, 114.0, 101.0, 56.8; HRMS [M + H; ESI-ORBITRAP] calcd for C₈H₈BrN₂O (as free base): 226.9820; found: 226.9813.

1-(4-Benzoylpiperazin-1-yl)-2-(7-bromo-4-methoxy-1H-pyrrolo[2,3-c]pyridin-3-yl)ethane-1,2-dione, 23. To a slurry of AlCl₃ (3.75 g, 28.1 mmol, 4.3 equiv) in DCM (14 mL) at 0 °C was added bromide 21 (2.00 g, 92 wt %, 6.50 mmol, 1.0 equiv), followed by a mixture of DCM (2.6 mL) and nitromethane (3.2 mL). After 20 min, methyl oxalyl chloride (1.60 g, 13.0 mmol, 2.0 equiv) was added, and the resulting reaction mixture was further stirred at 0 °C until reaction was complete by HPLC analysis (typically 5 h). The reaction crude was then slowly added into a biphasic mixture of THF (30 mL) and aqueous solution of Na₂SO₄ (1.0 M, 30 mL) which was precooled with an ice/water bath. The organic phase was collected. After washing with water (30 mL), the organic crude was distilled with constant water addition until residual nitromethane was <7% (mol/mol to the ester intermediate) by NMR analysis. To the resulting slurry of the methyl ester was added aqueous NaOH (10.0 N, 2.3 mL, 3.5 equiv). After the complete saponification, the resulting sodium salt was acidified by a slow addition of aqueous HBr solution (48%, 3.7 mL) at 45 °C, leading to the crystallization of the product as its HBr salt. The resulting slurry was cooled to 21 °C over 3 h. The product was filtered, washed with aqueous HBr solution (0.5 M, 10 mL), and dried under vacuum at 50 °C to provide the oxalate as its HBr salt (1.97 g, 79% yield). Melting point (mp) = 107 °C; ¹H NMR (400 MHz, DMSO-*d*₆) δ : 13.04 (s, 1 H), 11.34 (s, br, 2 H), 8.34 (s, 1 H), 7.82 (s, 1 H), 3.92 (s, 3 H); ¹³C NMR (100 MHz, DMSO-*d*₆) δ : 182.8, 166.2, 149.9,

137.6, 133.0, 123.6, 121.6, 116.8, 114.0, 56.2. IR (KBr, cm⁻¹) 3297, 3159, 1688, 1557, 1419, 1166, 1125, 978, 889, 756, 702, 636; HRMS [M + H; ESI-ORBITRAP] calcd for C₁₀H₈BrN₂O₄: 298.9667; found: 298.9678.

To the HBr salt of the oxalic acid derivative (5.03 g, limiting reagent) and dimethylformamide (68 mL) was stirred vigorously at ambient temperature until a homogeneous solution formed. The solution was cooled to 10 °C, at which point 1,1'-carbonyl diimidazole (3.46 g, 1.7 equiv) was added. After stirring at 10 °C for 3 h, benzoylpiperazine hydrochloric salt (3.70 g, 1.3 equiv) was added, and the mixture was warmed to 25 °C and stirred at 25 °C until reaction reached completion by HPLC monitoring (typically 2 h). The reaction was quenched with water (10 mL) and warmed up to 40 °C. Additional water (70 mL) was slowly added to enable the crystallization of amide 23. After cooling to 25 °C, the slurry was held at 25 °C for 10 h, then filtered, and washed with dimethylformamide/water (1:1 v/v, 15 mL). The solid was collected, reslurried with water/tetrahydrofuran (10:1 v/v, 25 mL), rinsed with tetrahydrofuran (15 mL, 3 mL/g), and dried at 60 °C in a vacuum to afford 1-(4-benzoylpiperazin-1-yl)-2-(7-bromo-4-methoxy-1H-pyrrolo[2,3-c]pyridin-3-yl)ethane-1,2-dione 23 as a tan solid (5.49 g, 92 wt %, 85.2% yield). HPLC at 230 nm using Ascentis Express C18, 2.7 μ m, 4.6 \times 150 mm column following gradient method 0% B (0 min) to 30% B (5 min) to 45%B (20 min) to 100%B (25 min) then 100% B (30 min). Mobile phase A: water (80%), methanol (20%) with 0.01 M NH₄OAc. Mobile phase B: acetonitrile (75%), methanol (15%), water (5%) with 0.01 M NH₄OAc, retention time: 10.55 min. Melting point (mp) = 252.5 °C; ¹H NMR (500 MHz, CDCl₃) δ : 8.31 (s, 1H), 7.84 (s, 1H), 7.45 (s, br, 5H), 3.94 (s, 3H), 3.66 (s, br, 4H), 3.40 (s, br, 4H); ¹³C NMR (1250 MHz, CDCl₃) δ : 185.4, 169.3, 166.2, 149.9, 138.3, 135.5, 133.2, 129.7, 128.4 (2), 127.1 (2), 123.8, 121.1, 116.9, 114.9, 56.8, 45.1 (2, br), 40.5 (2, br); HRMS [M + H; ESI-ORBITRAP] calcd for C₂₁H₂₀BrN₄O₄: 471.0662; found: 471.0654.

Lithium 3-(2-(4-benzoylpiperazin-1-yl)-2-oxoacetyl)-4-methoxy-7-(3-methyl-1H-1,2,4-triazol-1-yl)pyrrolo[2,3-c]pyridine-1-ide, potassium bromide, 25. To a mixture of amide 23 (12 g, 22.656 mmol) and acetonitrile (96 mL) at 20 °C was added 3-methyl-1H-1,2,4-triazole 17 (2.83 g, 33.98 mmol), followed by aqueous potassium hydroxide (45 wt %, 5.93 g, 47.58 mmol), water (4.08 g, 226.56 mmol), and *N,N'*-dimethyl-1,2-cyclohexanediamine (4.92 g, 33.98 mmol). The overall mixture was stirred at 20 °C for 1 h before adding copper(I) iodide (0.863 g, 4.53 mmol). The reaction mixture was heated to 75 °C and stirred until reaction reached completion by HPLC monitoring (typically 18 h). The mixture was cooled to 45 °C and diluted with acetonitrile (264 mL). At 45 °C, the crude slurry was washed with a solution of EDTA (6.70 g, 22.66 mmol) in 45 wt % aqueous potassium hydroxide (2 \times , 60 mL), followed by 45 wt % aqueous potassium hydroxide (45 mL). The organic crude was distilled at constant volume until KF reached <1.3 wt %. The resulting solution was cooled to 30 °C and filtered to remove inorganic particulates. The liquors were then further concentrated to ca. 240 mL. Water was added to the concentrated mixture until a KF of 4.5 wt % was achieved. Lithium bromide (2.102 g, 24.22 mmol) was added, at which point the lithium salt of 25 readily crystallized out the solution. After aging overnight, the solids were collected by filtration, washed sequentially with acetonitrile/water (98/2 v/v, 65 mL) and then acetonitrile (44 mL), and dried at 45 °C under vacuum. Azaindole 25 was obtained as a pale yellow solid (8.94 g, 14.94 mmol, 66% yield). ¹H NMR (400 MHz, DMSO-*d*₆) δ : 9.51 (s, 1 H), 8.07 (s, 1 H), 7.56 (s, 1 H), 7.44 (br s, 5 H), 3.87 (s, 3 H), 3.62 (m, 4 H), 3.38 (m, 4 H), 2.38 (s, 3 H); ¹³C NMR (100 MHz, DMSO-*d*₆) δ : 169.29, 168.68, 159.46, 149.46, 144.76, 138.02, 135.61, 133.62, 129.64, 128.42, 127.06, 125.66, 119.15, 113.42, 56.75, 13.79; HRMS [M + H; ESI-ORBITRAP] calcd for C₂₄H₂₃N₇O₄: 474.1884; found: 474.1876. Li: 1.49 wt %; calcd for C₂₄H₂₂BrKLiN₇O₄: 1.16 wt %; K: 6.82 wt %; calcd for C₂₄H₂₂BrKLiN₇O₄: 6.53 wt %.

3-(2-(4-benzoylpiperazin-1-yl)-2-oxoacetyl)-4-methoxy-7-(3-methyl-1H-1,2,4-triazol-1-yl)-1H-pyrrolo[2,3-c]pyridin-1-yl)-methyl di-*tert*-butyl phosphate, 26. To a 125 mL reactor equipped with an overhead stirbar was charged azaindole 25 (12.5 g

[Limiting Reagent], 20.34 mmol), potassium phosphate tribasic (comilled, 0.045 in. mesh) (4.32 g, 20.35 mmol, 1.0 equiv), and tetraethylammonium iodide (2.61 g, 10.15 mmol, 0.50 equiv). Sequentially acetonitrile (KF = 0.85%, 63.5 mL) and a solution of phosphate **27** in DCM (1.48 M, 17.9 mL, 26.52 mmol, 1.3 equiv) were added, and the resulting mixture was warmed to 40–45 °C. After 21 h, the reaction mixture was concentrated to ~30 mL. Dichloromethane (50 mL) was added, followed by phosphoric acid (0.2 M in water, 60 mL). The lower DCM layer was collected and washed with phosphoric acid (0.2 M in water, 70 mL) and then water (70 mL). IPAc (40 mL) was added to the DCM solution, and the resulting solution distilled at 35 °C to remove DCM, while additional IPAc (100 mL) was added to effect a constant volume distillation. Once the distillation was complete, the mixture was cooled to 20 °C over 1.5 h and aged overnight. The product was filtered, washed sequentially with IPAc (50 mL) and MTBE (50 mL), and dried in vacuum oven at 50 °C to give phosphate **26** as a white solid (8.59 g, 61% yield). Melting point (mp) = 198–202 °C; ¹H NMR (400 MHz, CDCl₃) δ: 8.51 (s, 1 H), 8.17 (s, 1 H), 7.88 (s, 1 H), 7.39 (br s, 5 H), 5.92 (d, J = 16 Hz, 2 H), 4.03 (s, 3 H), 3.90–3.35 (m, 8 H), 2.47 (s, 3 H), 1.25 (s, 18 H); ¹³C NMR (100 MHz, CDCl₃) δ: 184.56, 170.50, 165.81, 161.56, 150.66, 145.34, 141.79, 134.86, 130.05, 129.52, 128.53, 127.46, 126.96, 124.64, 122.55, 115.07, 83.70 (d, J = 8 Hz), 73.54 (J = 6 Hz), 56.82, 45.88, 41.55, 29.47, 29.43, 13.80; HRMS [M + H; ESI-ORBITRAP] calcd for C₃₃H₄₃N₇O₈P: 696.2911; found: 696.2885.

■ ASSOCIATED CONTENT

■ Supporting Information

Copies of ¹H/¹³C NMR spectra and HPLC chromatograms for new compounds. This material is available free of charge via the Internet at <http://pubs.acs.org>.

■ AUTHOR INFORMATION

Corresponding Author

*E-mail: martin.eastgate@bms.com.

Present Address

[†]Boehringer Ingelheim Pharmaceuticals, Inc., 900 Ridgebury Rd, Ridgefield, CT 06877, United States.

Notes

The authors declare no competing financial interest.

■ ACKNOWLEDGMENTS

The authors would like to thank Drs. David Kronenthal, Rajendra Deshpande, Rodney Parsons, and Robert Waltermire for support, Prof. Phil Baran, Prof. Marty Burke, Dr. Nicolas Cuniere, and Dr. Wendel Doubleday for useful discussions, Dr. Qi Gao for X-ray crystallography, and Dr. Charles Pathirana and Mr. Michael Peddicord for assistance with characterization.

■ REFERENCES

- (1) Wyatt, R.; Kwong, P. D.; Desjardins, E.; Sweet, R. W.; Robinson, J.; Hendrickson, W. A.; Sodroski, J. G. *Nature* **1998**, 393, 705.
- (2) (a) Wang, T.; Zhang, Z.; Meanwell, N. A.; Kadow, J. F.; Yin, Z.; Xue, Q. M.; Reguerio-Ren, A.; Matiskella, J. D.; Ueda, Y.; US 20040110785, June 10, 2004. (b) Ueda, Y.; Connolly, T. P.; Kadow, J. F.; Meanwell, N. A.; Wang, T.; Chen, C.-P. H.; Yeung, K.-S.; Zhang, Z.; Leahy, D. K.; Pack, S. K.; Soundararajan, N.; Sirard, P.; Levesque, K.; Thoraval, D.; US 20050209246, September 22, 2005.
- (3) Bristol-Myers Squibb R&D Home Page; <http://www.bms.com/research/investigational/HIV/Pages/BMS-663068.aspx>, accessed July 2014.
- (4) Li, Z.; Zhou, N.; Sun, Y.; Ray, N.; Lataillade, M.; Hanna, G. J.; Krystal, M. *Antimicrob. Agents Chemother.* **2013**, 57, 4172.
- (5) Soundararajan, N.; Qiu, Y.; Hu, W.; Kronenthal, D. K.; Sirard, P.; Lajeunesse, J.; Droghini, R.; Chidambaram, R.; Qian, X.; Natalie, K. J.; Pack, S. K.; Reising, N.; Tang, E.; Fakes, M. G.; Gao, Q.; Qian, F.;

Vakkalagadda, B. J.; Lai, C.; Kuang, S.-M.; US 20060293304, December 28, 2006.

(6) Tripp, J. C.; Fanfair, D. D.; Schultz, M. J.; Murugesan, S.; Fox, R. J.; Chen, C.-P. H.; Ivy, S. E.; Payack, J. F.; Doubleday, W. W.; WO 2012106189, August 9, 2012.

(7) (a) Bartoli, G.; Palmieri, G.; Bosco, M.; Dalpozzo, R. *Tetrahedron Lett.* **1989**, 30, 2129. (b) Bartoli, G.; Bosco, M.; Dalpozzo, R.; Palmieri, G.; Marcantoni, E. *J. Chem. Soc., Perkin Trans. 1.* **1991**, 2757.

(8) (a) Blaazer, A. R.; Lange, J. H. M.; van der Neut, M. A. W.; Mulder, A.; den Boon, F. S.; Werkman, T. R.; Kruse, C. G.; Wadman, W. J. *Eur. J. Med. Chem.* **2011**, 46, S086. (b) Ganser, C.; Lauermann, E.; Maderer, A.; Stauder, T.; Kramb, J.-P.; Plutizki, S.; Kindler, T.; Moehler, M.; Dannhardt, G. *J. Med. Chem.* **2012**, 55, 9531.

(9) (a) Huestis, M. P.; Fagnous, K. *Org. Lett.* **2009**, 11, 1357. (b) Hands, D.; Bishop, B.; Cameron, M.; Edwards, J. S.; Cottrell, I. F.; Wright, S. H. B. *Synthesis* **1996**, 877.

(10) (a) Sakamoto, T.; Satoh, C.; Kondo, Y.; Yamanaka, H. *Heterocycles* **1992**, 34, 2379. (b) Mahadevan, I.; Rasmussen, M. J. *Heterocycl. Chem.* **1992**, 29, 359.

(11) Whelligan, D. K.; Thomson, D. W.; Taylor, D.; Hoelder, S. J. *Org. Chem.* **2010**, 75, 11.

(12) Eastgate, M. D.; Bultman, M. S.; Chen, K. C.; Fanfair, D. D.; Fox, R. J.; La Cruz, T. E.; Mudryk, B. M.; Risatti, C. A.; Simpson, J. H.; Soumeillant, M. C.; Tripp, J. C.; Xiao, Y.; US 20130203992, August 8, 2013.

(13) Wengryniuk, S. E.; Weickgenannt, A.; Reiher, C.; Strotman, N. A.; Chen, K.; Eastgate, M. D.; Baran, P. S. *Org. Lett.* **2013**, 15, 792.

(14) (a) Ullmann, F.; Bielecki, J. *Chem. Ber.* **1901**, 34, 2174. (b) Ullmann, F. *Chem. Ber.* **1903**, 36, 2382. (c) Ullmann, F.; Sponahel, P. *Chem. Ber.* **1905**, 38, 2211. (d) Goldberg, I. *Chem. Ber.* **1906**, 39, 1691.

(15) DeAmici, M.; DeMicheli, C.; Platini, F.; Della Bella, D.; Caramazza, I. *Eur. J. Med. Chem.* **1988**, 23, 511.

(16) Pictet, A.; Spengler, T. *Chem. Berichte* **1911**, 44, 2030.

(17) Fodor, G.; Nagubandi, S. *Tetrahedron* **1980**, 10, 1279.

(18) (a) Chang, M.-Y.; Tai, H.-Y. *Heterocycles* **2011**, 83, 2373. (b) Silveira, C.; Bernardi, A.; Kaufman, T. *Synlett* **2002**, 6, 907.

(19) Hock, H.; Lang, S. *Ber. Dtsch. Chem. Ges.* **1944**, 77, 257.

(20) Fife, W. J. *Org. Chem.* **1983**, 48, 1375.

(21) (a) Cobb, R. L.; McEwen, W. E. *Chem. Rev.* **1955**, 55, 511.

(b) Keith, J. M. *J. Org. Chem.* **2010**, 75, 2722.

(22) Banerjee, S.; Zeller, M.; Bruckner, C. J. *Org. Chem.* **2009**, 74, 4283.

(23) El-Faham, A.; Albericio, F. *Chem. Rev.* **2011**, 111, 6557.

(24) Londregan, A. T.; Jennings, S.; Wei, L. *Org. Lett.* **2011**, 13, 1840.

(25) Kato, Y.; Okada, S.; Tomimoto, K.; Mase, T. *Tetrahedron Lett.* **2001**, 42, 4849.

(26) Bromination of bis-methoxy azaindole **3** with POBr₃ could be accomplished in 50% yield using freshly distilled POBr₃ (6 equiv) in anisole at 130 °C.

(27) Sugimoto, O.; Mori, M.; Tanji, K.-I. *Tetrahedron Lett.* **1999**, 40, 7477.

(28) Lazzaroni, R.; Pini, D.; Bertozzi, S.; Fatti, G. *J. Org. Chem.* **1986**, 51, 505.

(29) Wengryniuk, S. E.; Weickgenannt, A.; Reiher, C.; Strotman, N. A.; Chen, K.; Eastgate, M. D.; Baran, P. S. *Org. Lett.* **2013**, 15, 792.

(30) Jones, G. O.; Liu, P.; Houk, K. N.; Buchwald, S. L. *J. Am. Chem. Soc.* **2010**, 132, 6205.

(31) For a synthesis of the N-benzoyl piperidine see: Hendrick, C. E.; McDonald, S. L.; Wang, Q. *Org. Lett.* **2013**, 15, 3444.

(32) For a synthesis of the triazole see: Faridoun Hussein, W. M.; Vella, P.; Ul Islam, N.; Ollis, D. L.; Schenk, G.; McGeary, R. P. *Bioorg. Med. Chem. Lett.* **2012**, 22, 380.

(33) (a) Klapars, A.; Huang, X.; Buchwald, S. L. *J. Am. Chem. Soc.* **2002**, 124, 7421. (b) Antilla, J. C.; Klapars, A.; Buchwald, S. L. *J. Am. Chem. Soc.* **2002**, 124, 11684.

(34) Shafir, A.; Buchwald, S. L. *J. Am. Chem. Soc.* **2006**, 126, 8742.

- (35) (a) Goodbrand, H. B.; Hu, N. X. *J. Org. Chem.* **1999**, *64*, 670.
(b) Kiyomori, A.; Marcoux, J.-F.; Buchwald, S. L. *Tetrahedron Lett.* **1999**, *40*, 2657.
- (36) Xie, X.; Chen, Y.; Ma, D. *J. Am. Chem. Soc.* **2006**, *128*, 16050.
- (37) Zheng, B.; Fox, R. J.; Sugiyama, M.; Fritz, A.; Eastgate, M. D. *Org. Process Res. Dev.* **2014**, *18*, 636.
- (38) Zheng, B.; Sugiyama, M.; Eastgate, M. D.; Fritz, A.; Murugesan, S.; Conlon, D. A. *Org. Process Res. Dev.* **2012**, *16*, 1827.
- (39) Hoffman, R. W.; Bruckner, D. *New J. Chem.* **2001**, *25*, 369.